ELSEVIER

Contact angle studies on anodic porous alumina

Rocío Redón [a,*], A. Vázquez-Olmos [a], M.E. Mata-Zamora [a], A. Ordóñez-Medrano [b],
F. Rivera-Torres [b], J.M. Saniger [a]

[a] *Centro de Ciencias Aplicadas y Desarrollo Tecnológico, Universidad Nacional Autónoma de México, Cd. Universitaria A.P. 70-186, C.P. 04510,
Coyoacán, México, D.F., Mexico*
[b] *Instituto de Investigaciones en Materiales, Universidad Nacional Autónoma de México, Cd. Universitaria, Cto. Exterior, S/N, C.P. 04510,
Coyoacán, México, D.F., Mexico*

Abstract

The preparation of nanostructures using porous anodic aluminum oxide (AAO) as templates involves the introduction of dissolved materials into the pores of the membranes; one way to determine which materials are preferred to fill the pores involves the measurement of the contact angles (θ) of different solvents or test liquids on the AAOs. Thus, we present measurements of contact angles of nine solvents on four different AAO sheets by tensiometric and goniometric methods. From the solvents tested, we found dimethyl sulfoxide (DMSO) and N,N'-dimethylformamide (DMF) to interact with the AAOs, the polarity of the solvents and the surfaces being the driving force.
© 2005 Elsevier Inc. All rights reserved.

1. Introduction

Nanoscale materials have been widely studied due to their singular properties and potential applications. In particular, one-dimensional (1D) nanoscale materials have attracted much attention in recent years [1]. One of the most important methods for the preparation of 1D nanoscale materials is the template technique, which uses nanoporous membranes as templates [2–4]. In this method, anodic aluminum oxide membranes (AAO), prepared by electrochemical etching of aluminum foil in oxalic, sulfuric, and phosphoric acid solutions are the membranes most commonly used [5–10] for the fabrication of semiconductor nanowires, superconductor nanowire arrays, carbon nanotube arrays, etc. These materials have been fabricated mainly by electro [11–13] and electroless [14] deposition, chemical vapor deposition [15], and sputtering or evaporating of the material on the surface of the AAO at high temperatures [16,17]; however, attempts to fill the pores by gravity alone have resulted unfruitful. Therefore, it is important to perform careful studies of liquid–solid interface interactions on the nanoscale in order to understand how the interfacial properties affect the introduction of molecules into the pores of membranes. To do so, the contact angle (θ) has been used as a measure of wetting between a liquid and a solid surface. Two main techniques are commonly used for studying contact angles on a flat solid surface: (a) The tensiometric or Wilhelmy method measures the forces that are present when a sample of solid is brought into contact with a solvent. A particular case of the tensiometric method is the Washburn technique, which is employed when the solid sample contains a porous structure or is a powder. In this method, the solid is brought into contact with the testing liquid and the mass of liquid absorbed into the solid is measured as a function of time [18,19]. (b) In the goniometric method, the contact angle can be assessed directly by measuring the angle formed between the solid and the tangent to the drop surface. The present investigation involves the use of these techniques.

* Corresponding author. Fax: +52 55/5622 8651.
E-mail address: rredon@servidor.unam.mx (R. Redón).

Thus, following our interest [20–22] in the properties and structure of anodic alumina oxide membranes (AAO), we would like to report our findings on the measurement of the wetting properties of different solvents toward different AAOs.

2. Experimental

2.1. Materials

All chemicals, unless specified otherwise, were purchased from Aldrich Chemical Co. and used as received, without further purification. The following test liquids were used: 2-propanol (99.5%), 1-butanol (99.4%), acetone (99.66%), ethyl acetate (99.5%), acetonitrile (99.5%), N,N-dimethylformamide (DMF) (99.8%), dimethyl sulfoxide (DMSO) (99.9%), hexane (98.5%), benzene (99%) and ultrapure water (18 MΩ cm^{-1}) obtained from a Barnsted E-pure deionization system.

The solvents tested were chosen according to their polarity. *Polar solvents* have large dipole moments (μ_{solv}) and high dielectric constants ($\varepsilon_{r(solv)}$); *polar protic solvents* have at least one hydrogen atom bonded to either an oxygen or a nitrogen. This creates a polar molecule that will attract other molecules or ions using hydrogen bonding, as in water (H$_2$O), alcohols (R–O–H) (butanol, 2-propanol), or amines (R–NH$_2$). *Polar aprotic solvents* exhibit a molecular dipole moment but their hydrogen atoms are not bonded to oxygen or nitrogen atoms. Examples of such solvents include aldehydes (R–CHO), esters (R–COOR$'$) (ethyl acetate), ketones (R–CO–R$'$) (acetone), dimethyl sulfoxide (DMSO), and N,N'-dimethylformamide (DMF). Finally, *nonpolar solvents* present low dipole moments and small dielectric constants; examples include all the hydrocarbons— alkanes, alkenes, and alkynes (hexane, toluene). Table 1 shows the selected solvents and their values of dielectric constant, dipole moment, and surface tension (η_{solv}).

2.2. Instruments

The film surface was studied by scanning electron microscopy (SEM) in a JEOL JSM-5900LV microscope. Contact angle measurements by the tensiometric and Washburn methods were carried out using a Sigma 70 precision tensiometer produced by KSV Instruments. The goniometric determinations were carried out using a goniometer Ramé-Hart Inc. Model 100/07/00.

2.3. Template preparation

AAO templates were prepared using the fabrication procedures reported by us and other research groups [5–7,20–22]. In this case, aluminum sheets (99.999%) (20 × 10 mm, thickness 0.13 mm) were annealed under air at 480 °C for 60 min and mechanically and electrochemically polished

(1:5 v/v of EtOH/HClO$_4$) prior to anodization. The prepared sheets were then anodized at 40 and 20 V in 0.3 M aqueous oxalic or sulfuric acid solutions, respectively, at 10 °C, resulting in an average pore diameter for the AAO template of about 46 and 15 nm, respectively. The pore length obtained by this technique exceeds the 30-μm average. In order to enlarge the pores, the sheets were placed in aqueous phosphoric acid solution (0.35 M, $T = 30$ °C, $t = 10$ min); thus the average pore diameters obtained for the AAO template were 52 and 26 nm, respectively, the length of the pores remaining the same (about 30 μm). The pore size diameter and length were determined by SEM micrographs. See Table 2.

Fig. 1 shows the surface morphology of the AAO templates, before and after pore enlargement, analyzed by scanning electron microscopy (SEM).

2.4. Contact angle measurements

The prepared AAO sheets were used to measure the contact angle. In the *Wilhelmy method*, the samples were immersed to a set depth as the probe advanced into the liquid; data were collected and used to calculate an advancing contact angle (θ_{adv}). This process was reversed and, as the probe retreated from the liquid, data were collected and used to calculate the receding contact angle (θ_{rec}). In the *Washburn technique*, the sheets were brought into contact with the testing liquid and the mass of liquid absorbed into the solid was measured as a function of time, working at room temperature and immersion depth 18.88 mm, for all samples. In the *goniometric method*, contact angles (θ) were measured with sessile solvent drops. Nearly all measurements were made with drops that had a total volume of 10 μl. Advancing contact angles were measured from drops after sequential deposition. For the measurement of the receding contact angles, solvent was withdrawn. The AAO sheets were dried at 100 °C in a closed oven for 1 h after treatment with each sol-
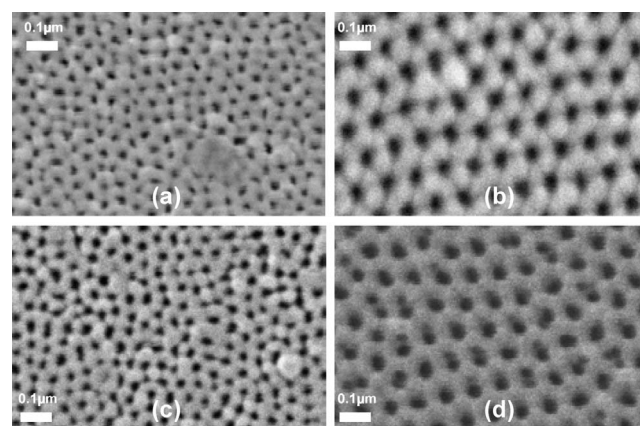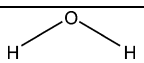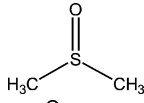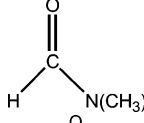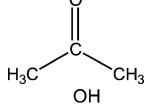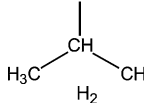

Fig. 1. SEM micrographs of the top view of anodic alumina sheets. Anodization was conducted in (a) 0.3 M sulfuric acid at 10 °C and 20 V (sample **1**) and (b) 0.3 M oxalic acid at 10 °C and 40 V (sample **3**). Pore opening was carried out in 0.35 M phosphoric acid at 30 °C for 10 min for (c) sulfuric acid anodized (sample **2**) and (d) oxalic acid anodized (sample **4**).

Table 1
Test liquids properties

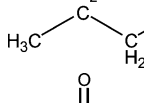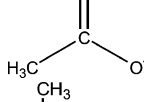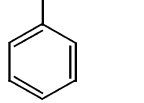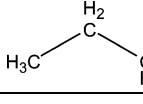| Test liquid	Structure	μ_{solv} (Debye)	$\varepsilon_{r(solv)}$[a] (8.85 pF/m)	γ_{solv} (mN/m)	η_{solv}[b] (mPa s)
Water		1.85	80.0	73.0	1.00
DMSO		3.96	47.2	25.0	2.20
DMF		3.82	38.3	25.0	0.92
Acetone		2.88	20.7	23.7	0.30
2-Propanol		1.68	20.1	23.8	2.86
Butanol		1.66	17.8	24.6	2.95
Ethyl acetate		1.78	6.02	23.9	0.46
Toluene		0.36	2.4	28.5	0.59
Hexane		0	2.02	18.43	0.31

[a] The dielectric constants of the solvents are given relative to the dielectric constant of a vacuum, 8.85 F/m. (Information provided by http://www.cartage.org.lb/en/themes/Sciences/Chemistry/Electrochemis/TheoryElectrolytes/Units/Units.htm.)

[b] η_{solv} = viscocity.

Table 2
Conditions for the template preparation and average pore diameter

Sample	Acid solution	Temperature (°C)	Voltage (V)	Pore enlarging conditions	Average pore diameter (nm)
1	0.3 M sulfuric acid	10	20	–	15
2	0.3 M sulfuric acid	10	20	0.35 M H_3PO_4, 30 °C, 10 min	26
3	0.3 M oxalic acid	10	40	–	46
4	0.3 M oxalic acid	10	40	0.35 M H_3PO_4, 30 °C, 10 min	52

vent and allowed to reach room temperature in a desiccator for 1 h extra before the next solvent was used.

3. Results and discussion

3.1. Wilhelmy method

The interaction between the liquid and the surface can be estimated by contact angle (θ) measurements. The details of the interaction between the surface and the solvents were explored by analysis of the effect of the properties of the liquid on the equilibrium contact angle (θ_{eq}) with the different surfaces. The θ_{eq} values were determined from the intersection of the fits for advancing and receding angles versus contact angle hysteresis ($\Delta\theta$, which is the difference between the advancing and the receding angles) with the ordinate at $\Delta\theta = 0$, one finds the equilibrium angle θ_{eq} [23]. Fig. 2 presents the plots of ethyl acetate contact angle as a function of the dynamic hysteresis for one of the AAOs (sample 2). Table 3 summarizes the results for all four AAOs.

If the equation

$$\cos\theta_{eq} = 0.5(\cos\theta_{adv} + \cos\theta_{rec}), \qquad (1)$$

Table 3
Contact angle tensiometric measurements, experimental (θ_{eq}) and arithmetic mean data ($0.5(\cos\theta_{adv} + \cos\theta_{rec})$)

| Test liquid	Sample **1**		Sample **2**		Sample **3**		Sample **4**	
	θ_{eq}	$0.5(\theta_{adv} + \theta_{rec})$	θ_{eq}	$0.5(\theta_{adv} + \theta_{rec})$	θ_{eq}	$0.5(\theta_{adv} + \theta_{rec})$	θ_{eq}	$0.5(\theta_{adv} + \theta_{rec})$
Water	68.1 ± 0.3	77.5 ± 0.3	65.8 ± 0.0	78.2 ± 0.2	73.3 ± 0.1	82.2 ± 0.4	62.6 ± 0.2	81.6 ± 0.3
DMSO	32.7 ± 0.3	26.2 ± 0.2	36.9 ± 0.3	35.3 ± 0.3	50.6 ± 0.1	56.0 ± 0.6	48.5 ± 0.1	54.2 ± 0.4
DMF	36.6 ± 0.3	40.1 ± 0.6	45.7 ± 0.4	45.0 ± 0.3	56.2 ± 0.1	56.8 ± 0.2	54.4 ± 0.3	54.6 ± 0.6
Acetone	57.8 ± 0.1	57.3 ± 0.3	59.3 ± 0.4	61.3 ± 0.4	63.7 ± 0.2	63.7 ± 0.6	67.6 ± 0.1	67.8 ± 1.2
2-Propanol	63.3 ± 0.2	62.3 ± 0.2	53.5 ± 0.8	63.3 ± 0.2	69.2 ± 0.0	68.7 ± 0.2	69.5 ± 0.3	69.5 ± 0.2
Butanol	61.2 ± 0.1	58.2 ± 0.5	60.8 ± 0.1	61.6 ± 1.0	67.3 ± 0.1	66.5 ± 0.3	66.6 ± 0.0	67.0 ± 0.3
Ethyl acetate	59.1 ± 0.3	58.2 ± 0.3	59.9 ± 0.0	61.2 ± 0.3	67.4 ± 0.4	66.8 ± 0.6	64.5 ± 0.4	65.1 ± 0.3
Toluene	61.9 ± 0.3	63.9 ± 0.5	58.3 ± 0.4	62.6 ± 0.5	68.9 ± 0.1	68.4 ± 0.1	69.0 ± 0.1	69.2 ± 0.4
Hexane	57.9 ± 0.2	57.9 ± 0.2	59.2 ± 0.8	61.4 ± 0.7	64.5 ± 0.3	66.1 ± 0.4	68.0 ± 0.1	67.1 ± 0.5
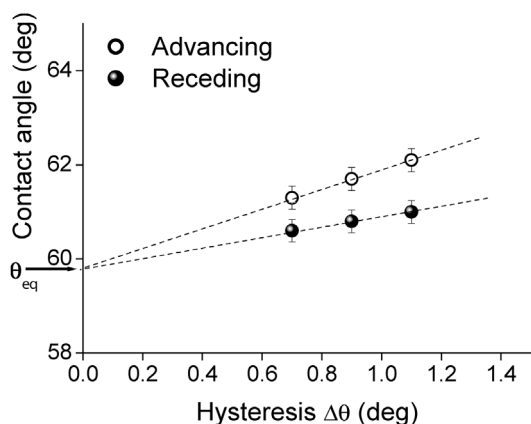
Fig. 2. Advancing (open circles) and receding (filled circles) contact angles vs contact angle hysteresis for ethyl acetate on sample **2**. The dashed lines correspond to the linear regressions. The equilibrium contact angle is 59.9 in this case.
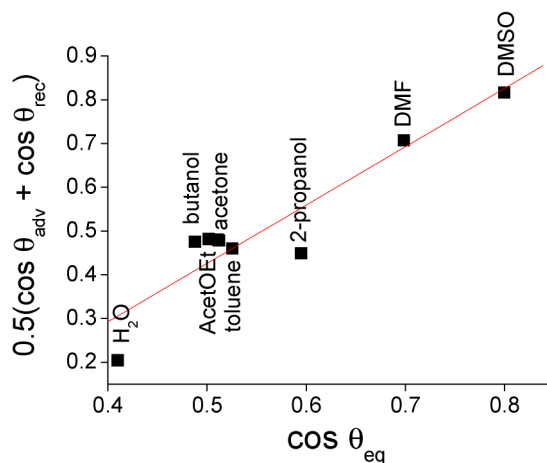

Fig. 3. Comparison between arithmetic mean cosine $0.5(\cos\theta_{adv} + \cos\theta_{rec})$ data vs experimental $\cos\theta_{eq}$ data for sample **2**.

(a)

(b)

Fig. 4. Effect of $\varepsilon_{r(solv)}$ (a) and μ_{solv} (b) on the contact angle (θ_{eq}) obtained with the dynamic tensiometric method.

where the terms adv and rec stand for advancing and receding [24], is used to calculate θ_{eq} using the θ_{adv} and θ_{rec} data obtained in the present investigation, the θ_{eq} values thus obtained are very similar to those obtained experimentally, see Table 3 and Fig. 3. The tendencies and results discussed further are the same with both values.
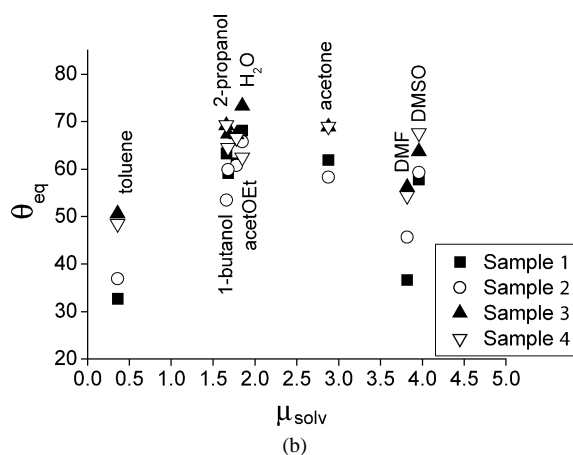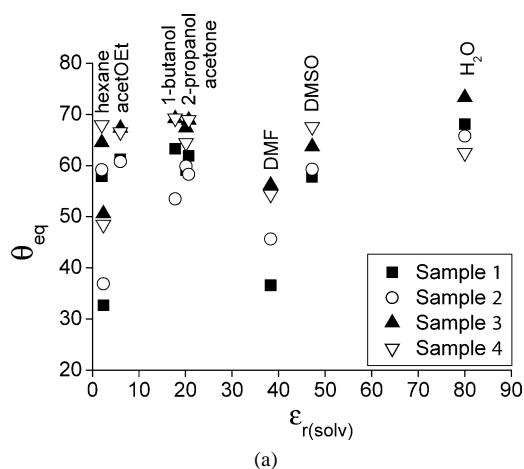
As will be discussed further, the most definitive and meaningful properties affecting the θ_{eq} were the dielectric constants and the dipolar moments of the solvents, as is shown in Fig. 4.

Table 3 shows the experimental values of θ_{eq} obtained for samples **1** to **4**. A general inspection of the θ_{eq} values shows that DMSO and DMF, in this order, are the solvents that best wet the porous anodic aluminum oxide sheets. On the other hand, for a given solvent, the sulfuric AAOs have a lower
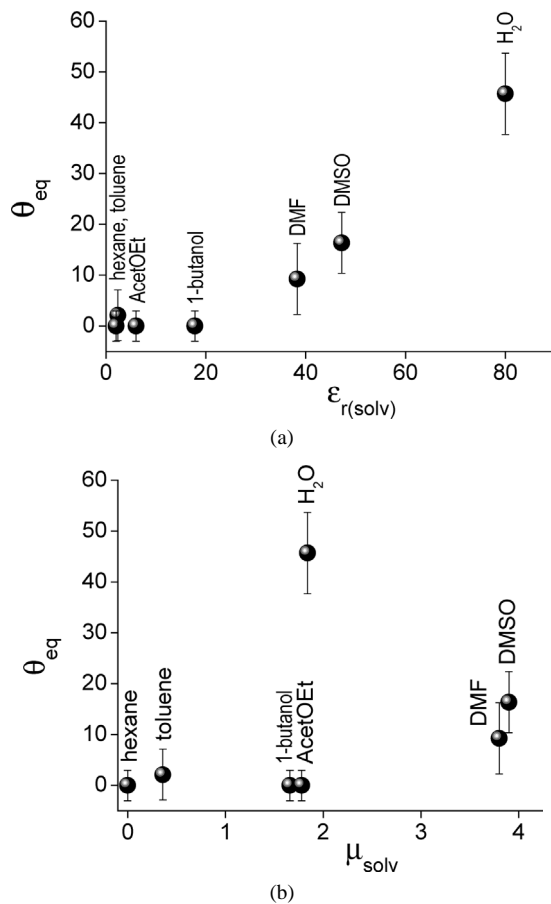
Fig. 5. Effect of $\varepsilon_{r(solv)}$ (a) and μ_{solv} (b) on the goniometric contact angle for sample **1**.

Fig. 6. Effect of $\varepsilon_{r(solv)}$ (a) and μ_{solv} (b) on the contact angle obtained with the Washburn method for sample **1**.

θ_{eq} than the oxalic AAOs; thus, it can be concluded that the influence of the widening is less significant than the type of alumina. The highest θ_{eq} values are systematically obtained for the case of water. Thus, it seems clear that water, due to its high surface tension value, practically does not wet any of the samples. These findings have practical importance and clearly show the convenience of using DMSO and DMF as solvents for an easier filling of the anodic alumina pores, as well as the inherent difficulty of introducing aqueous solutions into the pores.

The θ_{eq}'s for the four AAO sheets evaluated with the tensiometric method on the different test liquids are summarized in Table 3. Closer consideration of this group reveals that there is a dependence of the values of polar parameters (μ_{solv} and $\varepsilon_{r(solv)}$, Fig. 4) from solvents and surfaces. The main difference between the AAOs studied in this work is the surface composition, this is, the amount of hydroxide, sulfate, and oxalate groups formed during the anodized process. The AAO surfaces interact with the liquid phase via surface groups, thus, the polar component defines, in part, the strength of the interaction between the test liquid and the AAO surface [25]. None to medium polar tested solvents result in higher values of θ_{eq} and, thus, in a poorer interaction with the AAO surface. Water exhibits high val-
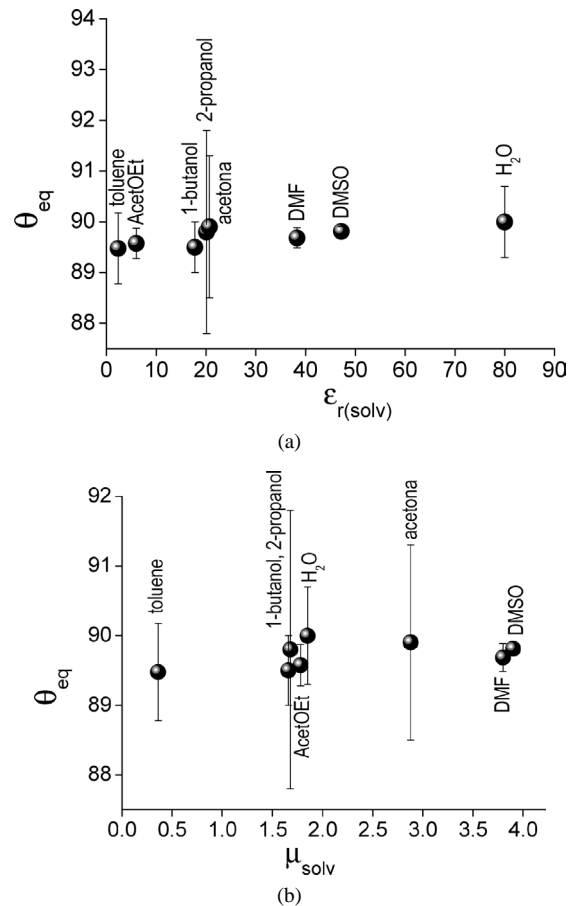
ues of $\varepsilon_{r(solv)}$ and μ_{solv}, but it also has the highest value of γ_{solv}, which results in the worst interaction with the AAO surface, whereas DMSO and DMF have the higher values of $\varepsilon_{r(solv)}$ and μ_{solv}, with $\gamma_{solv} = 25$. Therefore these solvents present stronger interactions with the surface groups, in particular with the hydroxide groups from the AAO surfaces, which can explain the observable values of θ_{eq} for these solvents. This interaction also exists in water but, once again, the high value of γ_{solv} prevents water from spreading to afford the highest θ_{eq} values. These results suggest that there is a delicate balance between the properties of the tested liquids and the high component on the dipolar contribution of the solvents and their surface tension, referred as "disjoining pressure" [26].

3.2. Goniometric and Washburn determinations

The θ_{eq} were evaluated using both goniometric and Washburn techniques (Figs. 5 and 6), with results given in Table 4. However, (i) goniometric measurements are extremely sensitive to variations in the local heterogeneity of the chemistry and topography of the surface, and this results in a large standard deviation in the experimental data, and the values of θ_{eq}, except for water, are too low (0°–10°), and

Table 4
Contact angle goniometric (G) and Washburn (W) measurements

Test liquid	θ_{eq}							
	Sample **1**		Sample **2**		Sample **3**		Sample **4**	
	G	W	G	W	G	W	G	W
Water	53.7 ± 6.2	89.5 ± 0.7	27.4 ± 10.2	90.0 ± 0.1	70.2 ± 10.1	89.9 ± 0.2	52.6 ± 5.5	89.5 ± 0.7
DMSO	18.1 ± 2.7	89.9 ± 0.1	14.3 ± 2.5	89.9 ± 0.2	21.5 ± 2.1	67.1 ± 1.3	24.4 ± 5.9	87.6 ± 0.8
DMF	9.9 ± 3.0	89.9 ± 0.2	8.4 ± 2.2	75.8 ± 1.0	14.6 ± 0.1	55.8 ± 3.1	14.9 ± 3.5	89.6 ± 0.6
Acetone	*	91.0 ± 1.4	*	88.5 ± 0.7	*	89.4 ± 0.8	*	87.0 ± 1.4
2-Propanol	0	87.5 ± 4.6	0	94.4 ± 1.9	69.2 ± 0.0	74.7 ± 1.8	*	89.0 ± 1.4
Butanol	0	20.4 ± 0.5	$2.3 \pm .4$	82.5 ± 2.2	4.1 ± 1.2	56.9 ± 1.6	25.9 ± 4.8	88.0 ± 1.4
Ethyl acetate	0	89.8 ± 0.3	0	92.7 ± 3.7	1.4 ± 0.4	75.2 ± 1.1	3.8 ± 1.2	89.6 ± 0.6
Toluene	1.5 ± 0.3	89.5 ± 0.7	3.8 ± 1.9	81.0 ± 1.4	4.3 ± 2.9	90.8 ± 0.4	12.8 ± 5.8	89.5 ± 0.8
Hexane	*	0	*	0	*	0	*	0

* Unable to measure.

(ii) the results obtained by the Washburn method reveal no spontaneous penetration into the pores for any of the applied liquids. Therefore, it is clear that these methods are inadequate and/or not sensible enough to analyze the effect of the contact angle on the nanopores of AAO surfaces.

3.3. Wetting of porous templates

Nanoscale wetting phenomena can be depicted by considering a small liquid droplet deposited on a smooth solid substrate; its wetting behavior can be described by the spreading parameter, defined as $S = \gamma_{sv} - \gamma_{sl} - \gamma_{lv}$ (with γ_{sv}, γ_{sl}, γ_{lv} respectively the solid–vapor, solid–liquid, and liquid–vapor interfacial tensions). If S is negative, a liquid drop deposited on the solid adopts an equilibrium shape corresponding to a finite contact angle θ_{eq} defined by Young's condition, $\cos\theta_{eq} = (\gamma_{sl} - \gamma_{sv})/\gamma_{lv}$; if S is positive, spontaneous spreading occurs, and the equilibrium situation corresponds to complete coverage of the solid by a thin liquid film. S measures the interfacial energy per unit area gained during the spreading [27]. Thus we propose the following explanation for the wetting of AAOs, the subject of study in the present investigation. If a liquid is allowed to spread on the pore walls of AAOs (Figs. 7a–7c), first the test liquid is brought into contact with the membrane (Fig. 7a). Organic materials and most solvents are considered as low-energy materials with respect to their surface energies, whereas inorganic materials are referred as high-energy materials (covalent, ionic, and metallic). Low-energy liquids spread rapidly on high-energy surfaces. Therefore, the pore walls will be covered by a mesoscopic film if they exhibit a high surface energy (Fig. 7b) [28]. We suggest that the underlying driving forces are due to short-range as well as long-range polar interactions between the wetting liquid and the pore walls. Thus, if the adhesive force (γ_{sl}) is strong enough to overcome the cohesive force (γ_{lv}), the pores will be completely filled, as in the cases of DMSO and DMF (Fig. 7c). In contrast, if the cohesive force is stronger than the adhesive, the equilibrium could be reached on a time scale from several months up to several years. This could be the case
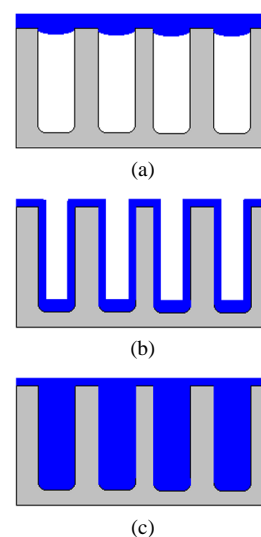

Fig. 7. Schematic representation of the different stages of pore wetting. (a) A test liquid is brought into contact with the AAO membrane and the liquid spreads on the substrate. (b) A mesoscopic film of the liquid rapidly wets the pore walls. (c) The liquid wetted the nanostructured layer.

of water. We have previously reported on the obtaining of nanostructures by immersion only, after 15 days [29].

The experimental results suggest that the water occupies only the very top of the nanopores, as is shown in Fig. 7a. Due to the lack of detailed structural information for the solid–liquid "nanointerface," this interpretation would need further investigation.

Despite the fact that the effect of the small differences between the values of θ_{eq} from the four AAO sheets can be ruled out by experimental error, an alternative explanation can be based on the number of anions on the surface. Since the widened process eliminates, in part, hydroxyl, sulfate, and/or oxalate anions [30,31], this would result in a less inorganic and polar surface, lowering the energy surfaces and so the liquid–solid interaction. Thus, the alumina that had been widened (**2** and **4**) had a poorer interaction with the test liquids than that not widened (**1** and **3**). Finally, alumina sheets **1** and **2** can be considered more polar than **3** and **4**, since the later have oxalate anions, in contrast with **1** and **2**, which contain sulfate anions on their surfaces.

4. Summary

Specific polar parameters were identified to describe the effect of the contact angle on porous anodic alumina oxide sheets. The best correlation was found between the polar contribution of the test liquids through $\varepsilon_{r(solv)}$ and μ_{solv} values and the equilibrium contact angle (θ_{eq}). The solvents DMSO and DMF have perfect equilibrium between polar and surface tension properties for complete filling of the porous surface, opposite to water, which has high values of $\varepsilon_{r(solv)}$ and μ_{solv}, but too high surface tension (γ_{solv}), thus preventing water from filling the pores, causing an increase in the contact angle value. Liquids with low $\varepsilon_{r(solv)}$ and μ_{solv} values do not completely fill the pores of the membranes and presented values of θ_{eq} around 60°. The wetting between sheets with or without widening is basically the same, that is, $\theta_{eq}(\mathbf{1}) \cong \theta_{eq}(\mathbf{3})$ and $\theta_{eq}(\mathbf{2}) \cong \theta_{eq}(\mathbf{4})$; but, between different anodized sheets, the θ_{eq} values are notably different, expressed as $\theta_{eq}(\mathbf{1} \text{ and } \mathbf{3}) < \theta_{eq}(\mathbf{2} \text{ and } \mathbf{4})$. These findings have practical importance and clearly show the convenience of using DMSO and DMF as a solvent for easier filling of the anodic alumina porous, as well as the inherent difficulty of introducing aqueous solutions into these pores.

Acknowledgments

References

[1] Q. Li, C. Wang, J. Am. Chem. Soc. 125 (2003) 9892.
[2] J.W. Elam, D. Routkevitch, P.P. Mardilovich, S.M. George, Chem. Mater. 15 (2003) 3507.
[3] W. Lung-Shen, L. Chi-Young, C. Hsin-Tien, Chem. Commun. (2003) 1964.
[4] L. Zhao, W. Yang, Y. Ma, J. Yao, Y. Li, H. Liu, Chem. Commun. (2003) 2442.
[5] K. Nishio, M. Nakao, A. Yokoo, H. Masuda, Jpn. J. Appl. Phys. 42 (2003) L83.
[6] T.T. Xu, R.D. Piner, R.S. Ruoff, Langmuir 19 (2003) 1443.
[7] S.G. Yang, T. Li, L.S. Huang, T. Tang, J.R. Zhang, B.X. Gu, Y.W. Du, S.Z. Shi, Y.N. Lu, Phys. Lett. A 318 (2003) 440.
[8] A.P. Li, F. Müller, A. Birner, K. Nielsch, U. Gösele, J. Appl. Phys. 84 (1998) 6023.
[9] N.M. Yakovleva, L. Anicai, A.N. Yakovlev, L. Dima, E.Y. Khanina, M. Buda, E.A. Chupakhina, Thin Solid Films 416 (2002) 16.
[10] N.M. Yakovleva, A.N. Yakovlev, E.A. Chupakhina, Thin Solid Films 366 (2000) 37.
[11] F. Muller, A.D. Muller, M. Kroll, G. Schmid, Appl. Surf. Sci. 171 (2001) 125.
[12] S.Z. Chu, K. Wada, S. Inoue, S.I. Todoroki, Y.K. Takahashi, K. Hono, Chem. Mater. 14 (2002) 4595.
[13] B.R. Martin, D.J. Dermody, B.D. Reiss, M. Fang, A. Luon, M.J. Natan, T.E. Mallouk, Adv. Mater. 11 (1999) 1021.
[14] V.P. Menon, C.R. Martin, Anal. Chem. 6 (1995) 1920.
[15] K.B. Shelimov, D.N. Davydov, M. Moskovits, Appl. Phys. Lett. 77 (2000) 1722.
[16] L. Meng-Ke, L. Mei, K. Ling-Bin, G. Xin-Yong, L. Hu-Lin, Mater. Sci. Eng. A 354 (2003) 92.
[17] M.J. Alfonso, M. Menéndez, J. Santamaría, Catal. Today 56 (2000) 247.
[18] E.W. Washburn, Phys. Rev. 17 (1921) 273.
[19] Z. Peršin, K. Stana-Kleinshek, T. Kreže, Croat. Chem. Acta 75 (2002) 271.
[20] Y.C. Sui, J.M. Saniger, Mater. Lett. 48 (2001) 127.
[21] Y.C. Sui, J.A. Gonzalez-Leon, A. Bermudez, J.M. Saniger, Carbon 39 (2001) 1709.
[22] Y.C. Sui, D.R. Acosta, J.A. Gonzalez-Leon, A. Bermudez, J. Feuchtwanger, B.Z. Cui, J.O. Flores, J.M. Saniger, J. Phys. Chem. B 105 (2001) 1523.
[23] H. Kamusewitz, W. Possart, D. Paul, Colloids Surf. A 156 (1999).
[24] E. Wolfram, R. Faust, in: J.F. Padday (Ed.), Wetting, Spreading and Adhesion, Academic Press, London, 1978, p. 213.
[25] O.K. Varghese, D. Gong, M. Paulose, K.G. Ong, C.A. Grimes, E.C. Dickey, J. Mater. Res. 17 (2002) 1162.
[26] V.M. Starov, Adv. Colloid Interface Sci. 39 (1992) 147.
[27] D. Ausserré, A.M. Picard, L. Léger, Phys. Rev. Lett. 57 (1986) 2671.
[28] M. Steinhart, J.H. Wendorff, R.B. Wehrspohn, Chemphyschem 4 (2003) 1117.
[29] R. Redón, M.E. Mata-Zamora, A. Vázquez-Olmos, J.M. Saniger, submitted for publication.
[30] H. Takahashi, K. Fijimoto, H. Konno, M. Nagayama, J. Electrochem. Soc. 131 (1984) 1856.
[31] Y. Yamamoto, N. Baba, Thin Solid Films 101 (1983) 329.